

Edge of Chaos as Critical Local Symmetry Breaking in Dissipative Nonautonomous Systems

Ricardo Chacón

*Departamento de Física Aplicada, E.I.I., Universidad de Extremadura, Apartado Postal 382,
06006 Badajoz, Spain and Instituto de Computación Científica Avanzada (ICCAEx),
Universidad de Extremadura, 06006 Badajoz, Spain*

(Dated: December 3, 2024)

The fully nonlinear notion of resonance—*geometrical resonance*—in the general context of dissipative systems subjected to *nonsteady* potentials is discussed. It is demonstrated that there is an exact local invariant associated with each geometrical resonance solution which reduces to the system’s energy when the potential is steady. The geometrical resonance solutions represent a *local symmetry* whose critical breaking leads to a new analytical criterion for the order-chaos threshold. This physical criterion is deduced in the co-moving frame from the local energy conservation over the shortest significant timescale. Remarkably, the new criterion for the onset of chaos is shown to be valid over large regions of parameter space, thus being useful beyond the perturbative regime and the scope of current mathematical techniques.

Hamiltonian and dissipative systems have traditionally been studied separately due to their clearly different dynamic properties¹: dissipation forces give rise to the existence of transient dynamics associated with the basins of the different attractors, while the Poincaré integral invariants of Hamiltonian systems lead to special behaviour of the eigenvalues of equilibria and periodic orbits, and to existence theorems for various types of orbits such as the celebrated Kolmogorov-Arnold-Moser theorem. To date, only the notion of geometrical resonance (GR)² has been able to provide a deep link between autonomous Hamiltonian and non-autonomous dissipative systems in the sense that it offers a universal procedure with which to locally “Hamiltonianize” an otherwise dissipative system by suitably choosing the non-autonomous term(s) $f_i(t)$ such that the system’s energy is conserved locally: $f_i(t) = f_{i,GR}(t)$. The original formulation of GR analysis was for *steady* potentials², and was applied to diverse nonlinear problems involving such potentials^{3–11}, including the stability of the responses of an overdamped bistable system⁷, the suppression of spatio-temporal chaos and the stabilization of localized solutions in general spatio-temporal systems^{5,8–10}, quantum control in trapped Bose-Einstein condensates (BECs)¹¹, and the characterization of periodic solutions of a fractional Duffing’s equation¹².

On the other hand, a major body of research has considered *nonsteady* potentials appearing in different physical contexts such as synchrotron motion of beams¹², BECs in optical lattices¹⁴, electron transport in semiconductor superlattices¹⁵, and nanoscale devices powered by the lateral Casimir force¹⁶, just to cite a few representative examples. In general, the reference frames co-moving with nonsteady potentials are accelerating frames, which introduces an additional complexity into analysis of the dynamics relative to the laboratory reference frame (L-frame). Since GR is neither more nor less than a *local symmetry*, namely that the dynamics equations remain locally invariant under time reversal when the non-autonomous terms are suitably locally chosen, $f_i(t) = f_{i,GR}(t)$, it seems appropriate and pertinent to explore its implications in general systems.

In this paper, new properties of this subtle symmetry in the generalized context of dissipative systems in nonsteady potentials are characterized and exploited to determine a physical criterion for the order-chaos threshold in parameter space whose accuracy and scope goes beyond current perturbative mathematical techniques. The theory is discussed through the universal model of a particle subjected to a spatially periodic and temporally shaken potential which describes, for example, the chaotic phase oscillation of a proton beam in a cooler synchrotron¹³.

Results

Theory

Let us consider the class of non-autonomous dissipative systems

$$\ddot{x} = g(x, t) - d(x, \dot{x}), \quad (1)$$

where the overdot denotes d/dt , $g(x, t) \equiv -\partial V(x, t)/\partial x$, with $V(x, t) \equiv V[x - f(t)]$ being a nonsteady and spatially periodic potential while $f(t)$ is an *a priori* arbitrary function of time, and where $-d(x, \dot{x})$ is a generic dissipative force. In the potential reference frame (V-frame) with $z(t) = x(t) - f(t)$, Eq. (1) reads

$$\ddot{z} = g(z) - d(z, \dot{z}, f, \dot{f}, t) - \ddot{f}. \quad (2)$$

In general, if $z_{GR}(t)$ is a GR solution of Eq. (2), it must satisfy

$$\ddot{z}_{GR} = g(z_{GR}), \quad (3)$$

$$\ddot{f}_{GR} = -d(z_{GR}, \dot{z}_{GR}, f_{GR}, \dot{f}_{GR}, t), \quad (4)$$

and hence

$$x_{GR} \equiv z_{GR} + f_{GR} \quad (5)$$

is a GR solution of Eq. (1) for a given set of initial conditions $[x_0 \equiv x(t=0), \dot{x}_0 \equiv \dot{x}(t=0)]$. Definitions (3)-(5) give rise to the following distinguishing properties. First, in contrast with the case of steady potentials², where f_{GR} is univocally determined from an algebraic equation involving the single GR solution associated with a given set of initial conditions, one has to solve a differential equation for f_{GR} in the present general case and obtain the initial values $f_{GR}(t=0) \equiv f_{GR,0}, \dot{f}_{GR}(t=0) \equiv \dot{f}_{GR,0}$ as a part of the whole solution. This is because the GR scenario for nonsteady potentials involves *two* reference frames, the V-frame being non-inertial in the general case. Second, conditions (3)-(4) are equivalent to the local energy conservation requirement

$$(1/2)\dot{z}_{GR}^2 + V[z_{GR}] \equiv E_{GR} = const \quad (6)$$

in the V-frame, while one has the requirement of a different local invariant in the L-frame:

$$I_{GR} \equiv \frac{\dot{x}_{GR}^2}{2} + V[x_{GR} - f_{GR}] + \dot{f}_{GR} \left(\frac{\dot{f}_{GR}}{2} - \dot{x}_{GR} \right) = const. \quad (7)$$

After Taylor expanding the potential, the local invariant I_{GR} can be recast into the more transparent form

$$(1/2)\dot{x}_{GR}^2 + V[x_{GR} - f_{GR,0}] + S[x_{GR}, f_{GR}] = const, \quad (8)$$

where,

$$S[x_{GR}, f_{GR}] \equiv \sum_{n=1}^{\infty} \frac{(-1)^n}{n!} (f_{GR} - f_{GR,0})^n V^{(n)}[x_{GR} - f_{GR,0}] + \dot{f}_{GR} \left(\dot{f}_{GR}/2 - \dot{x}_{GR} \right), \quad (9)$$

with $V^{(n)} \equiv d^n V(z)/dz^n$. From Eq. (8) one sees that, under GR conditions, the energy associated with the corresponding steady potential is *not* (locally) conserved in the L-frame, as expected, while the new invariant I_{GR} allows the temporal evolution of this energy to be calculated for each GR solution. Third, in the Hamiltonian limiting case, i.e., $d(x, \dot{x}) \rightarrow 0$, Eq. (4) becomes $\ddot{f}_{GR} = 0$, and hence $f_{GR}(t) = Vt$ with V being an arbitrary constant and where an additional additive constant has been taken to be zero without loss of generality. This means that, in the absence of dissipation, GR solutions are solely possible for potentials traveling with constant speed, i.e., for inertial frames, as expected. And fourth, a GR solution will be observed if it is stable, i.e., if any small perturbation $\delta z(t)$ of $z_{GR}(t)$ is damped. After substituting $z(t) = z_{GR}(t) + \delta z(t)$ into Eq. (2) with $f(t) = f_{GR}(t)$, one obtains the linearized equation of motion for small perturbations $\delta z(t)$:

$$\ddot{\delta z} + \left(\frac{\partial d}{\partial \dot{z}} \right)_{GR} \dot{\delta z} + \left[\left(\frac{\partial d}{\partial z} \right)_{GR} - \left(\frac{dg}{dz} \right)_{GR} \right] \delta z = 0. \quad (10)$$

Note that this generalized Hill equation with dissipation also governs the stability of the GR solutions in the L-frame (cf. Eq. (5)). It is shown below that this stability analysis together with the dependence of the GR solutions on the system's parameters and the local invariants (6) and (8) allows one to get a new analytical criterion for the order-chaos threshold from the weakest useful approximation to the local energy conservation in the V-frame.

Universal model

To demonstrate the effectiveness of the present GR theory in a simple paradigmatic model, consider the dissipative dynamics of a particle subjected to a spatially periodic and temporally shaken potential:

$$\ddot{x} + \sin[x - f(t)] = -\eta\dot{x}. \quad (11)$$

The dimensionless Eq. (11) describes for example the pinion motion of a nanoscale device composed of a pinion and a rack coupled via the lateral Casimir force, where $\eta > 0$ is a damping coefficient while $f(t)$ accounts for the *a priori* arbitrary horizontal motion of the rack¹⁶. In the V-frame with $z(t) = x(t) - f(t)$, Eq. (11) reads

$$\ddot{z} + \sin z = -\eta\dot{z} - \eta\dot{f} - \ddot{f}. \quad (12)$$

Thus, GR solutions of Eq. (12) must satisfy

$$\ddot{z}_{GR} + \sin z_{GR} = 0, \quad (13)$$

$$\dot{z}_{GR} + \dot{f}_{GR} + \ddot{f}_{GR}/\eta = 0. \quad (14)$$

Exact analytical periodic solutions of the integrable pendulum (13)¹⁷ corresponding to libration and rotation motions are given by

$$\begin{aligned} z_{GR}^l(t; t_0, m) &= 2 \arcsin [\sqrt{m} \operatorname{sn}(t - t_0; m)], \\ \dot{z}_{GR}^l(t; t_0, m) &= 2\sqrt{m} \operatorname{cn}(t - t_0; m), \end{aligned} \quad (15)$$

and

$$\begin{aligned} z_{GR}^r(t; t_0, m) &= \pm 2 \operatorname{am}[(t - t_0)/\sqrt{m}; m], \\ \dot{z}_{GR}^r(t; t_0, m) &= \pm \frac{2}{\sqrt{m}} \operatorname{dn}\left[\frac{t - t_0}{\sqrt{m}}; m\right], \end{aligned} \quad (16)$$

respectively, where $\operatorname{sn}(\cdot; m)$, $\operatorname{cn}(\cdot; m)$, $\operatorname{dn}(\cdot; m)$, $\operatorname{am}(\cdot; m)$ are Jacobian elliptic functions of parameter $m \in]0, 1[$, the upper (lower) sign in the rotation solutions refers to counterclockwise

(clockwise) rotations, while t_0 is an arbitrary initial time. These solutions have the respective periods $T^l(m) \equiv 4K$ and $T^r(m) \equiv 2\sqrt{m}K$, where $K \equiv K(m)$ is the complete elliptic integral of the first kind¹⁸. Although the parameters corresponding to libration and rotation motions are inversely related each other, the same notation, m , is used here since both parameters are defined over the same interval¹⁷ and there is no possibility of confusion in the subsequent analysis. Also, definition $\text{sn}(\cdot; m) \equiv \sin[\text{am}(\cdot; m)]$ has been used to write a simpler alternative expression for $z_{GR}^r(t; t_0, m)$. After taking $t_0 = 0$ for simplicity, using the Fourier series of the Jacobian elliptic functions involved¹⁸, and integrating the linear differential equation (14), one straightforwardly obtains the GR excitations

$$\begin{aligned} f_{GR}^l(t) &\equiv C_1 + C_2 e^{-\eta t} + \sum_{n=0}^{\infty} b_n \cos(\omega_n t + \varphi_n), \\ f_{GR}^r(t) &\equiv C'_1 + C'_2 e^{-\eta t} \mp \frac{\pi t}{\sqrt{m}K} \pm \sum_{n=1}^{\infty} b'_n \cos(\omega'_n t + \varphi'_n), \end{aligned} \quad (17)$$

and the corresponding GR solutions in the L-frame

$$\begin{aligned} x_{GR}^l(t) &= C_1 + C_2 e^{-\eta t} + \sum_{n=0}^{\infty} \frac{b_n}{\text{tg } \varphi_n} \sin(\omega_n t + \varphi_n), \\ x_{GR}^r(t) &= C'_1 + C'_2 e^{-\eta t} \pm \sum_{n=1}^{\infty} \frac{b'_n}{\text{tg } \varphi'_n} \sin(\omega'_n t + \varphi'_n), \end{aligned} \quad (18)$$

with

$$\begin{aligned} b_n &\equiv \frac{2\pi\eta}{\omega_n K \sqrt{\eta^2 + \omega_n^2}} \text{sech} \left[\frac{(2n+1)\pi K'}{2K} \right], \\ b'_n &\equiv \frac{2\pi\eta}{\omega'_n K \sqrt{m} \sqrt{\eta^2 + \omega_n'^2}} \text{sech} \left(\frac{n\pi K'}{K} \right), \\ \omega_n &\equiv (n+1/2)\pi/K, \\ \omega'_n &\equiv n\pi/(\sqrt{m}K), \\ \varphi_n &\equiv \arctan(\eta/\omega_n), \\ \varphi'_n &\equiv \arctan(\eta/\omega'_n) \end{aligned} \quad (19)$$

and where $C_{1,2}, C'_{1,2}$ are constants to be determined from the initial conditions (x_0, \dot{x}_0) (see the Methods section), $K' \equiv K(1-m)$, while the upper (lower) sign in Eqs. (17) and (18) refers to counterclockwise (clockwise) rotations. These GR solutions have the following properties. (i) Their stability is governed by Eq. (10), i.e.,

$$\ddot{\delta z} + \eta \dot{\delta z} + \cos z_{GR}^{l,r} \delta z = 0, \quad (20)$$

which reduces to the Lamé equations

$$\frac{d^2 u}{dt^2} + [1 - \eta^2/4 - 2m \operatorname{sn}^2(t; m)] u = 0, \quad (21)$$

$$\frac{d^2 v}{d\tau^2} + [m(1 - \eta^2/4) - 2m \operatorname{sn}^2(\tau; m)] v = 0, \quad (22)$$

where $u = \exp(\eta t/2) \delta z$ and $v = \exp(\eta \sqrt{m} \tau/2) \delta z$ for librations and rotations, respectively. Standard results for these Lamé equations^{19,20} indicate that Eq. (20) presents only one instability region in the $m - \eta$ parameter plane. A careful comparison of Eq. (21) with Eq. (22) leads one to expect the instability region for librations to be clearly narrower than that for rotations owing to the term $m(1 - \eta^2/4) < 1 - \eta^2/4$ since $m \in]0, 1[$. Moreover, the maximum range of η values in the instability regions is expected to occur when $m \simeq 1$ for both kinds of motion due to all GR solutions $z_{GR}^{l,r}(t)$ converging to the separatrix (the most unstable phase path) of the integrable pendulum as $m \rightarrow 1$. Numerical simulations confirmed these expectations, as is shown in Fig. 1.

(ii) For any set of initial conditions not on the unperturbed separatrix, i.e., for *any* GR excitation (17) and corresponding solution (18), one sees that the dependence of *each* harmonic of such excitations and solutions on the damping coefficient has exactly the same form: $\eta/\sqrt{\eta^2 + \alpha}$, with α being a function of the corresponding natural period. From this it can be inferred that, for a periodic excitation $f(t)$ of amplitude γ , the dependence of the chaotic-threshold amplitude, γ_{th} , on η should obey this functional form *irrespective* of the value of η , an unanticipated result in view of the *perturbative* character of the current mathematical techniques to predict the onset of chaos (Melnikov's method (MM)). (iii) Since harmonic functions are commonly used to model periodic excitations, the GR solution corresponding to libration near the bottom of the potential well (i.e., $x_0 \approx 0, \dot{x}_0 \approx 0, m \gtrsim 0$) is of especial interest. One straightforwardly obtains the steady ($t \gg \eta^{-1}$) solutions (cf. Eqs. (17) and (18))

$$\begin{aligned} x_{GR}^l(t) &= 2\sqrt{m} \sin t + f_{GR}^l(t), \\ f_{GR}^l(t) &= \frac{2\sqrt{m}\eta}{\sqrt{1 + \eta^2}} \cos(t + \arctan \eta) + O(m^{3/2}), \end{aligned} \quad (23)$$

while the corresponding local invariant (8) reduces to

$$I_{GR}^l = (1/2) \dot{x}_{GR}^{l2}(t) - \cos x_{GR}^l(t) + \frac{f_{GR}^{l2}(t) + \dot{f}_{GR}^{l2}(t)}{2} + O(m^3), \quad (24)$$

i.e., $I_{GR}^l(t)$ is no more than the sum of the energy associated with the limiting case of steady potential plus the energy associated with the V-frame moving *as a linear harmonic oscillator of period 2π* , which is an unexpected result. (iv) In the Hamiltonian limiting case, i.e., $\eta \rightarrow 0$, GR

solutions for librations are not possible due to their oscillatory character around a fixed point is incompatible with the requirement of a traveling potential function (cf. third property in the previous subsection), while GR solutions for rotations are indeed possible (see Eq. (17)). (v) In the limit of very high dissipation ($\eta \rightarrow \infty$), the steady GR solutions are equilibria (cf. Eqs. (18) and (23)), as expected.

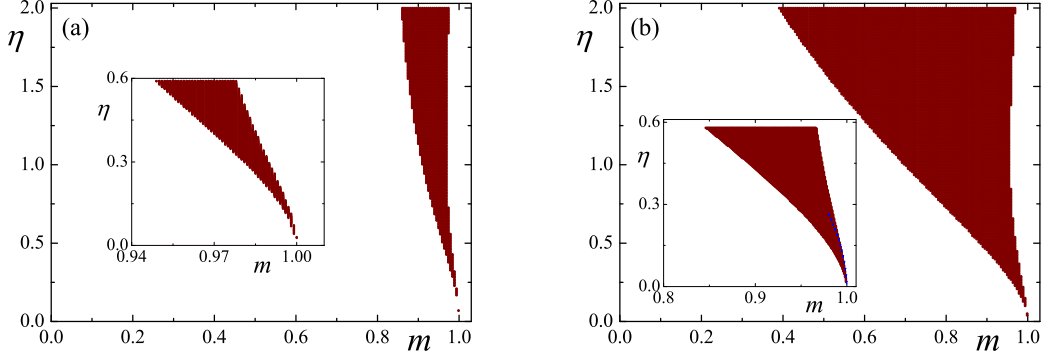


FIG. 1: **Stability-instability charts.** Stability-instability charts obtained by numerical integration of the Lamé's equations (a) Eq. (21) and (b) Eq. (22) for libration and rotation motions, respectively, where instability regions are indicated by dots. The insets show the tips of the instability tongues when $m \rightarrow 1$ and $\eta \rightarrow 0$.

Order-chaos threshold

Next, one can use the above properties of the GR solutions to obtain an analytical estimate of the order-chaos threshold associated with a generic T -periodic excitation $f_g(t)$ of amplitude γ . In general this generic excitation will not exactly correspond to any GR excitation function (17), and hence one cannot expect strict conservation (i.e., over an infinite timescale) of the invariants (6) and (7) for any set of initial conditions. Indeed, the energy flow is governed in the V-frame by the equation (cf. Eq. (12))

$$\frac{dE}{dt} = -\eta \dot{z}^2 - \eta \dot{z} \dot{f}_g - \dot{z} \ddot{f}_g. \quad (25)$$

For each set of initial conditions, the closer the excitation $f_g(t)$ is to the corresponding $f_{GR}(t)$, the smaller the deviation of the energy from the corresponding local invariant E_{GR} . Clearly, the weakest physical condition that will cope with this deviation is that the energy be locally conserved over the shortest significant timescale, i.e., as an average over a period of the corresponding GR

solution:

$$\left\langle \frac{dE}{dt} \right\rangle_{T^{l,r}}(t_0) \equiv \int_{-T^{l,r}/2}^{T^{l,r}/2} \left(\eta \dot{z}_{GR}^{l,r2} + \eta \dot{z}_{GR}^{l,r} \dot{f}_g + \dot{z}_{GR}^{l,r} \ddot{f}_g \right) dt = 0 \quad (26)$$

for some t_0 , and where $\dot{z}_{GR}^{l,r} \equiv \dot{z}_{GR}^{l,r}(t; t_0, m)$. Also, one assumes a *Galilean* resonance condition—a necessary condition for GR (cf. Eq. (14))—for both libration ($T = T^l/(2n+1)$ for some $n = 0, 1, \dots$) and rotation ($T = T^r/n$ for some $n = 1, 2, \dots$) motions. Thus, Eq. (26) provides a *local* condition that takes into account the initial phase difference between the generic excitation and the GR solution, hence allowing one to obtain a threshold condition (in particular, a threshold amplitude γ_{th}) for the energy conservation in its weakest sense. According to the above stability analysis, GR solutions are not uniformly stable as the natural period is varied. Therefore, Eq. (26) is subject to the caveat that it is not expected to be uniformly valid for all values of the excitation period because of its dependence on the integration domain. In the limiting case $T^{l,r} \rightarrow \infty$, when both libration and rotation GR solutions converge to the separatrix

$$\begin{aligned} z_{s,\pm}(t; t_0) &= \pm \arctan [\sinh(t - t_0)], \\ \dot{z}_{s,\pm}(t; t_0) &= \pm 2 \operatorname{sech}(t - t_0), \end{aligned} \quad (27)$$

the corresponding GR excitation is no longer a periodic function, as expected, but (for $t_0 = 0$)

$$f_{GR}^s(t) \equiv \tilde{C}_1 + \tilde{C}_2 e^{-\eta t} \mp 2 \operatorname{gd}(t) \pm 4 e^t \frac{{}_2F_1(1, \frac{1+\eta}{2}; \frac{3+\eta}{2}; -e^{2t})}{1+\eta}, \quad (28)$$

where $\tilde{C}_{1,2}$ are constants to be determined from the initial conditions (x_0, \dot{x}_0) (see the Methods section), $\operatorname{gd}(t)$ and ${}_2F_1(1, \frac{1+\eta}{2}; \frac{3+\eta}{2}; -e^{2t})$ are the Gudermannian and the hypergeometric functions, respectively²², and Eq. (26) becomes

$$\left\langle \frac{dE}{dt} \right\rangle_s(t_0) \equiv \int_{-\infty}^{\infty} \left(\eta \dot{z}_{s,\pm}^2 + \eta \dot{z}_{s,\pm} \dot{f}_g + \dot{z}_{s,\pm} \ddot{f}_g \right) dt = 0 \quad (29)$$

for some t_0 . Since the separatrix is the most unstable phase path, in the sense that it is the boundary between two *distinctly different* types of motions, one would expect the onset of chaos when a gradual breaking of the GR local symmetry reaches a critical value. Indeed, Eq. (29) provides the physical condition for such a critical breaking, hence allowing the order-chaos threshold in parameter space to be estimated. It should be stressed that, because the GR local symmetry is defined over the complete parameter space, condition (29) is postulated irrespective of the parameter values. For the sake of clarity, consider the application of condition (26) to the simple case of a harmonic excitation $f(t) = \gamma \cos(2\pi t/T)$. After some simple algebra (see the Methods

section), one straightforwardly obtains the following threshold amplitudes from Eq. (26):

$$\gamma_{th}^l = \frac{4\eta [E - (1 - m)K]}{\pi\omega\sqrt{\eta^2 + \omega^2} \operatorname{sech}(\omega K')}, \quad (30)$$

$$\gamma_{th}^r = \frac{4\eta\sqrt{m}E}{\pi\omega\sqrt{\eta^2 + \omega^2} \operatorname{sech}(\omega\sqrt{m}K')}, \quad (31)$$

where $\omega \equiv 2\pi/T$ and $E \equiv E(m)$ is the complete elliptic integral of the second kind¹⁸. Also, $\lim_{m \rightarrow 1} \gamma_{th}^{l,r} = \gamma_{th}^s$ with

$$\gamma_{th}^s = \frac{4\eta}{\pi\omega\sqrt{\eta^2 + \omega^2} \operatorname{sech}(\pi\omega/2)} \quad (32)$$

being the explicit estimate of the order-chaos threshold in parameter space.

Let us now compare the prediction (32) with that obtained from MM. In keeping with the assumptions of the MM^{23,1,21}, here it is assumed that one can write $\eta = \varepsilon\bar{\eta}$, $\gamma = \varepsilon\bar{\gamma}$ where $0 < \varepsilon \ll 1$ and $\bar{\eta}, \bar{\gamma}, \omega$ are of order unity. Next, one calculates the Melnikov function (MF), $M(t_0)$, for the system (12) with the harmonic excitation:

$$\ddot{z} + \sin z = -\varepsilon\bar{\eta}\dot{z} + \varepsilon\bar{\gamma}\omega^2 \cos(\omega t) + O(\varepsilon^2). \quad (33)$$

Since the MF provides an $O(\varepsilon)$ estimate of the distance between the stable and unstable manifolds of the perturbed system in the Poincaré section at t_0 , one readily obtains

$$M(t_0) = -8\eta \pm 2\pi\gamma\omega^2 \operatorname{sech}(\pi\omega/2) \cos(\omega t_0). \quad (34)$$

If the MF has a simple zero, then a homoclinic bifurcation occurs, signifying the appearance of homoclinic chaos²⁴. This yields the threshold value

$$\gamma_{th}^M = \frac{4\eta}{\pi\omega^2 \operatorname{sech}(\pi\omega/2)}. \quad (35)$$

Numerical simulations confirmed the effectiveness of estimate (32) as against (35). An illustrative example is shown in Fig. 2, in which one sees how the chaotic regions in the $\eta - \gamma$ parameter plane, determined by Lyapunov exponent (LE) calculations (see the Methods section), are reasonably well bounded by estimate (32), while the extrapolation (recall that η, γ must be much smaller than unity) of the MM estimate (35) clearly fails. Note that estimates (32) and (35) coincide for sufficiently small values of η (perturbative regime). This is not so surprising since the MF is, up to a constant, exactly the integral that Poincaré derived from Hamilton-Jacobi theory to obtain his celebrated obstruction to integrability²⁷, while the GR local symmetry implies a local restoration of integrability of an otherwise *non-integrable* system. Figure 3 shows illustrative examples of the

regularization routes as γ and η are changed while crossing the order-chaos threshold. Typically, the system (11) goes from a period-1 attractor to a strange chaotic attractor as the excitation amplitude increases for a sufficiently small value of the damping coefficient (see Fig. 3(a)). The overall evolution of the initial periodic state is characterized by the energy $E = \dot{x}^2/2 + 1 - \cos x$ undergoing a period-doubling route as γ is increased. Also, for fixed γ , the system (11) goes from the strange chaotic attractor existing at a sufficiently small value of the damping coefficient to a period-1 attractor as η is increased via an inverse period-doubling route (see Fig. 3(b)).

Discussion

In conclusion, a theory of geometrical resonance in dissipative systems subjected to nonsteady potentials has been presented, and its effectiveness in obtaining an analytical criterion for the order-chaos threshold in parameter space beyond the perturbative regime demonstrated by means of a paradigmatic example. From a theoretical point of view, the characterization and determination of the frontiers between chaotic and regular motions of real-world systems is a general problem that needs to be addressed in all branches of science. While the mathematical theory of deterministic chaos was definitively established by the work of Poincaré, Birkhoff, and Smale, the present physical theory suggests understanding the onset of homoclinic chaos as being coincident with a *critical breaking of the geometrical resonance local symmetry*, specifically, as coinciding with a critical breaking of the local conservation of the separatrix's energy in the co-moving frame for generic (periodic) nonsteady potentials. Finally, a natural continuation of the present work is the study of the geometrical resonance local symmetry and its eventual breakage in classical and quantum Hamiltonian systems.

Methods

Determination of the initial value problem. From Eqs. (13), (15), (16) with $t_0 = 0$, one obtains

$$\begin{aligned} f_{GR,0}^{l,r} &\equiv f_{GR}^{l,r}(t=0) = x_{GR}^{l,r}(t=0) - z_{GR}^{l,r}(t=0) = x_0, \\ \dot{f}_{GR,0}^l &\equiv \dot{f}_{GR}^l(t=0) = \dot{x}_{GR}^l(t=0) - \dot{z}_{GR}^l(t=0) = \dot{x}_0 - 2\sqrt{m}, \\ \dot{f}_{GR,0}^r &\equiv \dot{f}_{GR}^r(t=0) = \dot{x}_{GR}^r(t=0) - \dot{z}_{GR}^r(t=0) = \dot{x}_0 \mp \frac{2}{\sqrt{m}}, \end{aligned} \quad (36)$$

while from Eq. (18) one obtains

$$\begin{aligned} C_1 &= x_0 + \frac{1}{\eta} \left[\dot{x}_0 - \sum_{n=0}^{\infty} \frac{b_n \omega_n \cos^2 \varphi_n}{\sin \varphi_n} \right] - \sum_{n=0}^{\infty} b_n \cos \varphi_n, \\ C_2 &= \frac{1}{\eta} \left[-\dot{x}_0 + \sum_{n=0}^{\infty} \frac{b_n \omega_n \cos^2 \varphi_n}{\sin \varphi_n} \right], \end{aligned} \quad (37)$$

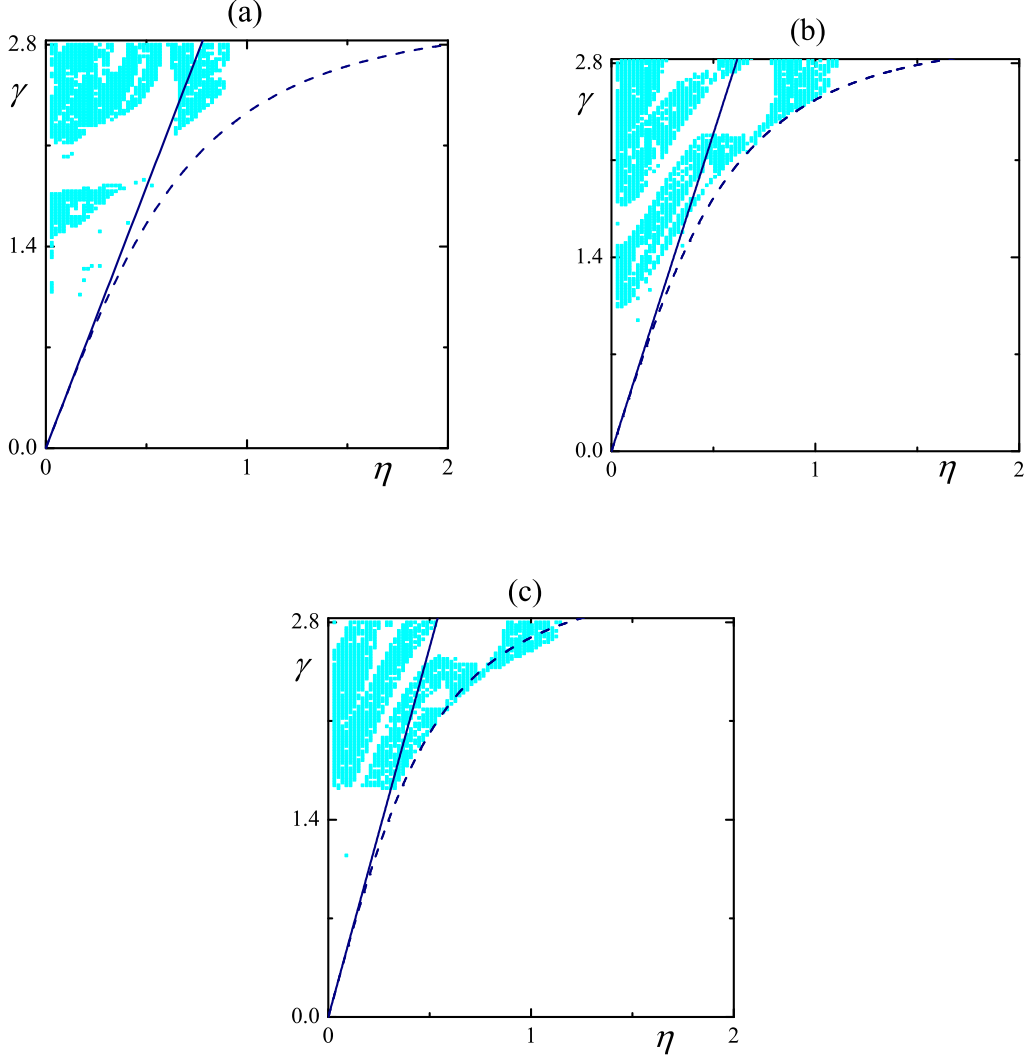


FIG. 2: **Chaotic regions in the control parameter plane.** Chaotic regions (dots) in the η – γ parameter plane corresponding to Eq. (11) with $f(t) = \gamma \cos(2\pi t/T)$ for three values of the driving period: **(a)** $T = 7.5$, **(b)** $T = 9.38$, **(c)** $T = 10.5$. A dot is plotted on a 100×140 grid when the corresponding maximal LE is greater than 10^{-3} . Dashed and solid lines represent the theoretical chaotic thresholds [cf. Eqs.(32) and (35), respectively] from GR analysis and MM, respectively.

for libration motions, and

$$C'_1 = x_0 + \frac{1}{\eta} \left[\dot{x}_0 \mp \sum_{n=1}^{\infty} \frac{b'_n \omega'_n \cos^2 \varphi'_n}{\sin \varphi'_n} \right] \mp \sum_{n=1}^{\infty} b'_n \cos \varphi'_n, \quad (38)$$

$$C'_2 = \frac{1}{\eta} \left[-\dot{x}_0 \pm \sum_{n=1}^{\infty} \frac{b'_n \omega'_n \cos^2 \varphi'_n}{\sin \varphi'_n} \right],$$

for rotation motions, and where $b_n, \omega_n, \varphi_n, b'_n, \omega'_n, \varphi'_n$ are given by Eq. (19), while the upper (lower)

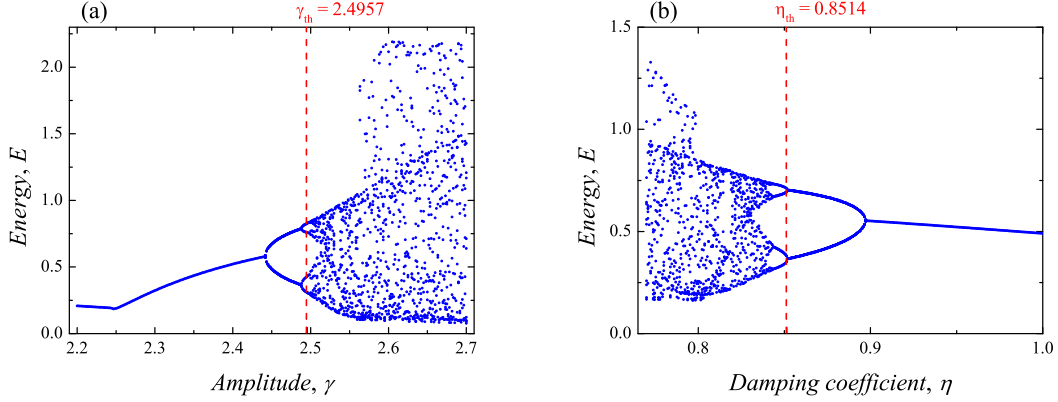


FIG. 3: **Bifurcation diagrams of Eq. (11) with $f(t) = \gamma \cos(2\pi t/T)$.** (a) Bifurcation diagram of energy $E = \dot{x}^2/2 + 1 - \cos x$ as a function of the amplitude γ for $\eta = 0.95$. The vertical dashed line indicate the threshold amplitude $\gamma_{th} = 2.4957$ predicted from Eq. (32). (b) Bifurcation diagram of energy $E = \dot{x}^2/2 + 1 - \cos x$ as a function of the damping coefficient η for $\gamma = 2.4$. The vertical dashed line indicate the threshold value of the damping coefficient $\eta_{th} = 0.8514$ predicted from Eq. (32). Fixed parameter: $T = 9.38$.

sign in Eqs. (36) and (38) refers to counterclockwise (clockwise) rotations.

Derivation of the geometrical resonance excitation for the separatrix. For the separatrix (27), Eq. (14) reduces to the linear differential equation

$$\ddot{f}_{GR}^s + \eta \dot{f}_{GR}^s = \mp 2\eta \operatorname{sech}(t). \quad (39)$$

After using the method of variation of parameters²⁵, one straightforwardly obtains the general solution given by Eq. (28) while its derivative is written

$$\dot{f}_{GR}^s(t) = -\tilde{C}_2 \eta e^{-\eta t} \mp 4\eta e^t \frac{{}_2F_1(1, \frac{1+\eta}{2}; \frac{3+\eta}{2}; -e^{2t})}{1+\eta}. \quad (40)$$

Finally, after taking into account (36) for $m = 1$, i.e., $f_{GR}^s(t=0) = x_0$, $\dot{f}_{GR}^s(t=0) = \dot{x}_0 \mp 2$, the integration constants are given by,

$$\begin{aligned} \tilde{C}_1 &= x_0 + \frac{1}{\eta} (\dot{x}_0 \mp 2), \\ \tilde{C}_2 &= \frac{1}{\eta} \left\{ -\dot{x}_0 \pm 2 \mp \eta \left[\psi\left(\frac{3+\eta}{4}\right) - \psi\left(\frac{1+\eta}{4}\right) \right] \right\}, \end{aligned} \quad (41)$$

where $\psi(\eta)$ is the psi (Digamma) function²², while the upper (lower) sign in Eqs. (28), (39), (40), and (41) refers to counterclockwise (clockwise) rotations.

Derivation of the threshold amplitudes for the onset of chaos. Let us consider the simple case of a harmonic excitation $f(t) = \gamma \cos(2\pi t/T)$.

Libration motions. Equation (26) for $T^l(m) \equiv 4K$ and the Galilean resonance condition $T = T^l/(2n+1), n = 0, 1, \dots$, reduces to

$$\left\langle \frac{dE}{dt} \right\rangle_{T^l}(t_0) = \int_{-2K}^{2K} \left[\eta \dot{z}_{GR}^{l2} - \eta \gamma \omega \dot{z}_{GR}^l \sin(\omega t) - \gamma \omega^2 \dot{z}_{GR}^l \cos(\omega t) \right] dt. \quad (42)$$

After substituting $\dot{z}_{GR}^l(t; t_0, m)$ from Eq. (15) into Eq. (42), using the Fourier series of the elliptic function $\text{cn}(\cdot; m)^{18}$, and using standard tables of integrals²⁸, one obtains the average energy over the period T^l as a function of the initial phase difference (ωt_0) between the harmonic excitation and the GR solution

$$\left\langle \frac{dE}{dt} \right\rangle_{T^l}(t_0) = 16\eta [E - (1-m)K] - 4\pi\gamma\omega\eta \text{sech}[\omega K'] \sin(\omega t_0) - 4\pi\gamma\omega^2 \text{sech}[\omega K'] \cos(\omega t_0). \quad (43)$$

From Eq. (43) one sees that a necessary condition for $\langle \frac{dE}{dt} \rangle_{T^l}(t_0)$ to change sign at some t_0 is written

$$16\eta [E - (1-m)K] \leq \sqrt{(4\pi\gamma\omega\eta \text{sech}[\omega K'])^2 + (4\pi\gamma\omega^2 \text{sech}[\omega K'])^2}, \quad (44)$$

where the equals sign in Eq. (44) yields the threshold amplitude γ_{th}^l given by Eq. (30).

Rotation motions. Equation (26) for $T^r(m) \equiv 2\sqrt{m}K$ and the Galilean resonance condition $T = T^r/n, n = 1, 2, \dots$, reduces to

$$\left\langle \frac{dE}{dt} \right\rangle_{T^r}(t_0) = \int_{-\sqrt{m}K}^{\sqrt{m}K} \left[\eta \dot{z}_{GR}^{r2} - \eta \gamma \omega \dot{z}_{GR}^r \sin(\omega t) - \gamma \omega^2 \dot{z}_{GR}^r \cos(\omega t) \right] dt. \quad (45)$$

After substituting $\dot{z}_{GR}^r(t; t_0, m)$ from Eq. (16) into Eq. (45), using the Fourier series of the elliptic function $\text{dn}(\cdot; m)^{18}$, and using standard tables of integrals²⁸, one obtains the average energy over the period T^r as a function of the initial phase difference (ωt_0) between the harmonic excitation and the GR solution

$$\left\langle \frac{dE}{dt} \right\rangle_{T^r}(t_0) = 8\eta\sqrt{m}E \mp 2\pi\eta\gamma\omega \text{sech}[\omega\sqrt{m}K'] \sin(\omega t_0) \mp 2\pi\gamma\omega^2 \text{sech}[\omega\sqrt{m}K'] \cos(\omega t_0), \quad (46)$$

where the upper (lower) sign in Eq. (46) refers to counterclockwise (clockwise) rotations. From Eq. (46) one sees that a necessary condition for $\langle \frac{dE}{dt} \rangle_{T^r}(t_0)$ to change sign at some t_0 is written

$$8\eta\sqrt{m}E \leq \sqrt{(2\pi\gamma\omega\eta \text{sech}[\omega\sqrt{m}K'])^2 + (2\pi\gamma\omega^2 \text{sech}[\omega\sqrt{m}K'])^2}, \quad (47)$$

where the equals sign in Eq. (47) yields the threshold amplitude γ_{th}^r given by Eq. (31).

Numerical simulations. Equations (11), (21), and (22) have been numerically solved using a fourth Runge-Kutta method with discrete time step $\delta t = 0.001$. Lyapunov exponents have been

computed using a version of the algorithm introduced in reference 26, with integration typically up to 2×10^4 drive cycles for each fixed set of parameters.

-
- [1] Lichtenberg, A. J. & Lieberman, M. A. *Regular and chaotic dynamics* (Springer-Verlag, Berlin, 1991).
 - [2] Chacón, R. Geometrical resonance as a chaos eliminating mechanism. *Phys. Rev. Lett.* **77**, 482-485 (1996).
 - [3] Chacón, R. Geometrical resonance in a driven symmetric bistable system subjected to strong or to weak damping. *Phys. Rev. E* **54**, 6153-6159 (1996).
 - [4] Chacón, R. Chaos and geometrical resonance in the damped pendulum subjected to periodic pulses. *J. Math. Phys.* **38**, 1477-1483 (1997).
 - [5] González, J. A., Mello, B. A., Reyes, L. I. & Guerrero, L. E. Resonance phenomena of a solitonlike extended object in a bistable potential. *Phys. Rev. Lett.* **80**, 1361-1364 (1998).
 - [6] Tereshko, V. & Shchekinova, E. Resonant control of the Rössler system. *Phys. Rev. E* **58**, 423-426 (1998).
 - [7] Chacón, R. Resonance phenomena in bistable systems. *International Journal of Bifurcation and Chaos* **13**, 1823-1829 (2003).
 - [8] González, J. A., Bellorín, A., Reyes, L. I., Vázquez, C. & Guerrero, L. E. Geometrical resonance in spatiotemporal systems. *Europhys. Lett.* **64**, 743-749 (2003).
 - [9] González, J. A., Bellorín, A., Reyes, L. I., Vázquez, C. & Guerrero, L. E. Pattern control and suppression of spatiotemporal chaos using geometrical resonance. *Chaos, Solitons and Fractals* **22**, 693-703 (2004).
 - [10] Raju, T. S. & Porsezian, K. On solitary wave solutions of ac-driven complex Ginzburg-Landau equation. *J. Phys. A: Math. Gen.* **39**, 1853-1858 (2006).
 - [11] Hai, W. H., Xie, Q. & Rong, S. G. Macroscopic quantum control of exact many-body coherent states. *Eur. Phys. J. D* **61**, 431-435 (2011).
 - [12] Jiménez, S., González, J. A. & Vázquez, L. Fractional Duffing's equation and geometrical resonance. *International Journal of Bifurcation and Chaos* **23**, 1350089 (2013).
 - [13] Ellison, M. et al. Driven response of the synchrotron motion of a beam. *Phys. Rev. Lett.* **70**, 591-594 (1993).
 - [14] Staliunas, K. & Longhi, S. Subdiffractive solitons of Bose-Einstein condensates in time-dependent optical lattices. *Phys. Rev. A* **78**, 033606 (2008).
 - [15] Balanov, A. G., Fowler, D., Patané, A., Eaves, L. & Fromhold, T. M. Bifurcations and chaos in semiconductor superlattices with a tilted magnetic field. *Phys. Rev. E* **77**, 026209 (2008).
 - [16] Ashourvan, A., Miri, M. & Golestanian, R. Noncontact rack and pinion powered by the lateral Casimir force. *Phys. Rev. Lett.* **98**, 140801 (2007).
 - [17] Whittaker, E. T. *A treatise on the analytical dynamics of particles and rigid bodies* (Cambridge U.P.,

- New York, 1937), 4th ed.
- [18] Byrd, P. F & Friedman, M. D. *Handbook of elliptic integrals for engineers and scientists* (Springer-Verlag, Berlin, 1971).
 - [19] Maier, R. S. Lamé polynomials, hyperelliptic reductions and Lamé band structure. *Phil. Trans. R. Soc. A* **366**, 1115-1153 (2008).
 - [20] Li, H. & Kusnezov, D. Group theory approach to band structure: scarf and Lamé Hamiltonians. *Phys. Rev. Lett.* **83**, 1283-1286 (1999).
 - [21] Guckenheimer, J. & Holmes, P. *Nonlinear oscillations, dynamical systems, and bifurcations of vector fields* (Springer-Verlag, New York, 1983).
 - [22] Abramowitz, M. & Stegun, I. A. *Handbook of mathematical functions* (Dover, New York, 1972).
 - [23] Melnikov, V. K. On the stability of the center for time periodic perturbations. *Trans. Mosc. Math. Soc.* **12**, 1-57 (1963).
 - [24] Poincaré, H. J. *Les méthodes nouvelles de la mécanique céleste* (Gauthier-Villars, Paris, 1899).
 - [25] Ince, E. L. *Ordinary differential equations* (Dover, New York, 1956).
 - [26] Wolf, A., Swift, J. B., Swinney, H. L. & Vastano, J. A. Determining Lyapunov exponents from a time series. *Physica D* **16**, 285-317 (1985).
 - [27] Poincaré, H. J. Sur le problème des trois corps et les équations de la dynamique. *Acta Mathematica* **13**, 1-270 (1890).
 - [28] Gradshteyn, I. & Ryzhik, I. *Table of Integrals, Series and Products* (Academic, New York, 1994)

Acknowledgements

The author thanks F. Balibrea, P. Binder, D. Farmer, E. Hernández-García, and P. J. Martínez for discussion and useful comments on an early version of the manuscript. This work was supported by the Ministerio de Economía y Competitividad (MECC, Spain) under Grant N° FIS2012-34902 and by the Junta de Extremadura (JEx, Spain) under Grant N° GR15146.